Article

On the Emergence of Spacetime and Matter from Model Sets

Marcelo Amaral [1]*, Fang Fang [1], Raymond Aschheim [1] and Klee Irwin [1]

[1] Quantum Gravity Research, Los Angeles, CA 90290, USA
* Correspondence: Marcelo@QuantumGravityResearch.org

Simple Summary: Starting from first principles and the mathematical structure of model set tiling spaces we propose a framework where the emergence of spacetime and matter can be addressed. The framework relies on a correspondence between short scale non-ergodic dynamics and large scale usual dynamics.

Abstract: We consider partition functions, in the form of state sums, and associated probabilistic measures for aperiodic substrates described by model sets and their associated tiling spaces. We propose model set tiling spaces as microscopic models for small scales in the context of quantum gravity. Model sets possess special self-similarity properties that allow us to consider implications on large and observable scales from the underlying (non-ergodic) dynamics. In particular we consider the implication of the underlying aperiodic substrate for the well known problem of time in quantum gravity, and propose a correspondence between small and large scales, the so-called ergodic correspondence, that addresses the emergence of matter properties and spacetime structure. In the process we find a possible bound in the mass spectrum of fundamental particles.

Keywords: Quantum Gravity; Problem of Time; Particle Physics; Emergence; Holographic Principle; Model Sets

1. Introduction

Emergence of spacetime geometry from underlying (Planck scale) discrete structures has been considered recently from different approaches such as entropic gravity [1,2], spin foams [3–5], causal dynamical triangulation [6,7], causal sets [8,9] and multiway hypergraph systems [10–13]. But no clear solution to the problem has been provided and we know little about the emergence of matter, in terms of particle and field properties [14], especially in a unified framework.

Regarding the emergence of spacetime geometry we can distinguish at least three slightly different approaches from the references above. First, the entropic gravity approach assumes emergence of gravity in a standard statistic mechanic and thermodynamic setup. Newton's law of gravitation and Einstein's field equations are derived from the holographic principle for arbitrary holographic screens enclosing huge numbers of matter configurations. Second, approaches such as causal sets and multiway hypergraphs study the appearance of the Riemannian geometry of general relativity in the continuum limit over more general discrete structures. Third, the approaches of spin foams (or more general loop quantum gravity) and causal dynamical triangulation look for the classical limit of quantized geometry after quantization of general relativity. Both approaches in this third category agree that the continuous geometric structures of general relativity should emerge at large scale from some classical or quantum underlying granularity.

In the spirit of causal sets and multiway hypergraph approaches we consider quasicrystals defined by the geometric cut-and-projection method in its most general form, called model sets [1] [15], as the underlying mathematical structure under which emergence can be addressed. Nevertheless the specific mechanism for emergence we propose is more related to the entropic gravity one. If we can understand the emergence of matter, then the entropic gravity approach can be used to understand the large scale gravity. In the literature of quasicrystal mathematics, model sets are usually developed as models for quasicrystal materials with good agreement with experiment [15,17–19]. For example, the free energy, among other observables, is shown to be invariant under translation of the window in perpendicular space, which gives a geometric understanding of the so-called phasons modes

[1] Some authors prefer the terminology of "cut and projection sets" but we agree with [16] on the priority and greater generality of the term "model sets" with regard to aperiodic structures and will use it from now on.

check for updates

Citation: . *Preprints* **2022**, *1*, 0. https://doi.org/

Received:
Accepted:
Published:

 doi:10.20944/preprints202111.0359.v2

[19]. Here we consider implications of the same mathematical structures on much smaller scales. The motivation for this proposal comes from different fronts, such as a renewed interest in discrete mathematics with regards to the quantum gravity regime as discussed in the references above, and the problem of time, where quasicrystals provide one interesting substrate to work with, which we will discuss later. We can also point out the fact that aperiodic structures appear in solutions of quantum cosmology both with general relativity and modified gravity theories [20] (and references therein) and that the grand unification program, which seeks to extend the standard model of particle physics to higher energy scales, relies heavily on large simple Lie algebraic structures, which are deeply related to quasicrystals through their root systems [21–23]. See also our recent work on a slightly different approach to quantum gravity [24] and references therein. More specifically, we will focus on quasicrystals derived from the E_8 root system. If the E_8 grand unified theory [25,26] can succeed, quasicrystals are a natural outgrowth of E_8 structures. Finally, self-similarity properties are a hallmark of quasicrystals and as we discuss later are good for problems involving multiple scales. We note that renormalization, relating physics at different scales, is an open problem in quantum gravity [5].

Our approach relies on the construction of a probabilistic measure over the model set tiling spaces, which allows us to compute the expectation values of observables. In statistical mechanics (classical or quantum) one in general relies on continuous symmetry invariance to guide the construction of probabilistic measures using the partition function from a Hamiltonian or a Lagrangian of the system under consideration. For discrete contexts one builds models such that the continuous structures can be recovered in a suitable limit. And there are also discrete symmetries which can be preserved, and which work as a guide in the same way as continuous symmetries. For example for lattice models one usually implements a partition function with discrete translation invariance. These kinds of model relying on translation symmetry are very successful in solid state physics with the well known Bloch and Floquet theories [27,28]. Quasicrystals posit a more general situation where there is no well-known procedure with regard to continuous/classical limits. Nevertheless, there are remarkable advances on building models implementing a particular model set scale invariance, which highlights the self-similar character of aperiodic structures, generalizing Bloch and Floquet theories from periodic to aperiodic structures [15,29]. We focus on the former situation of quasicrystals considered at small scales looking for some understanding of large scale physics in classical/continuous limits. This more general and less explored situation allows us to relax constraints on the construction of the partition function (and associated probabilistic measure) in terms of the underlying Hamiltonian or Lagrangian and to propose directly the partition function in terms of a state sum model [30,31]. State sums allow for constructing models which are an intermediate tool between the path integral for a continuous theory in quantum gravity and a lattice approximation of the same theory, because of the state sums independence of the discretization. Our construction of the state sum was guided only by the model set scale invariance coupled to general assumptions such as locality and superposition. In other words, we relax the ergodic hypothesis and consider a time average for observables not necessarily equal to the ensemble average from Gibbs' measures [32].

Accepting that the underlying model set's discrete structures does not necessarily follow the ergodic hypothesis allows us to postulate a correspondence between observables computed by usual quantum mechanics ensemble averages and the model set time averages under coarse graining. We propose that in the observation of physical properties such as the mass of particles, there is a limit in which the ergodic hypothesis should be recovered. Quantum theory such as the quantum field theory of the standard model of particle physics requires some parameters, like the mass, to be fixed by observation, which motivates the proposed correspondence, allowing us to address the emergence of some of those quantum observables such as the particles mass. In other words, if the short scale model set tiling space is seen as an internal structure of usual point like excitations, then time averaging the internal tiling space properties corresponds, in the limit of large numbers of tiling space points, to the ensemble average of the large scale system. The correspondence allows to get intrinsic properties from the model, instead of as external parameters.

Another implication to be considered by having different probabilistic measures for large and small scales is to use the small scale model set tiling spaces as a background for relativistic quantum

Preprints (www.preprints.org) | NOT PEER-REVIEWED | Posted: 23 March 2022 doi:10.20944/preprints202111.0359.v2

evolution. This background allows us to address the so-called problem of time in quantum gravity [33–36], which is the problem of implementing unitary quantum evolution in the absence of an absolute time parameter. We follow the usual program of considering relational evolution where some physical degree of freedom evolves relative to others. In this scenario we can distinguish three necessary notions of time, the usual background time parameter, the global monotonic relativistic one and a new notion of a clock variable [37]. We show that internal model set variables can play the role of a clock variable for relational evolution. A last related implication to be discussed is with regard to the emergence of spacetime structures such as inertia and the correspondence principle. We already mentioned the entropic gravity approach where geodesic motion of particles is understood as a result of an entropic force, a key element being the relationship between an accelerated frame of reference and temperature. We address the connection between acceleration and temperature for a given particle by proposing that a deviation from ergodicity leads to variation on emergent temperature, while at the same time leading to acceleration through the proposed ergodic correspondence.

This paper is organized as follows: in Section 2 we introduce the minimum concepts and definitions of model sets necessary for our discussion. In Section 3 we present the proposed state sum model, with associated probabilistic measure and expectation values, from the model set tiling spaces structures, which show the possibility of more general non-ergodic dynamics. In subsection 3.2 we present a novel method of model set embedding in a periodic lattice, which enables us to provide some explicit computations. The novel method is discussed in an explicit construction of a three-dimensional model set derived from the E_8 lattice. We present the implications in terms of the correspondence between quantum mechanical ensemble average observables and the model set time average ones, under coarse graining, and discuss the model set substrate playing the role of (internal) mass, inertia and clock for relational evolution in Section 4. We present our conclusions in Section 5. For self-consistency, we collect some results of model set theory, including the notion of tiling spaces, in Appendix A, and in Appendix B we present additional details on the novel method to describe model sets.

2. Model Sets Definitions

We start with some mathematical preliminaries for quasicrystals [15] relevant to our discussion. A cut-and-project scheme (CPS) is a 3-tuple $\mathcal{G} = \left(\mathbb{R}^d, G, \mathcal{L}\right)$, where $\mathbb{R}^d$ is a real euclidean space, G is some locally compact abelian group (in general it can be any topological group) and $\mathcal{L}$ is a lattice in $\mathbb{R}^d \times G$, with the two natural projections π:$\mathbb{R}^d \times G \to \mathbb{R}^d$ and $\pi_\perp$:$\mathbb{R}^d \times G \to G$, subject to the conditions that $\pi(\mathcal{L})$ is injective and that $\pi_\perp(\mathcal{L})$ is dense in G. $\mathcal{E} = \mathbb{R}^d \times G$ is the embedding space, the space $\mathbb{R}^d$ is called the parallel or physical space (the space of the model set) and G is the perpendicular or internal space. Together with a given CPS we need a non-empty relatively compact subset $K \subset G$ called the window or the coding set. With $L = \pi(\mathcal{L})$, for a given CPS π is a bijection between $\mathcal{L}$ and L. Then this scheme has a well-defined map, called star map, $\star : L \to G$:

$$x \mapsto x^\star := \pi_\perp(\pi_{\mathcal{L}}^{-1}(x)), \tag{1}$$

where $\pi_{\mathcal{L}}^{-1}(x)$ is the unique point in the set $\mathcal{L} \cap \pi^{-1}(x)$. The $\star$-image of L is denoted $L^\star$. From now on we will restrict the internal space to be another real euclidean space $G = \mathbb{R}^{d'}$.

For a given CPS $\mathcal{G}$ and a window K, model sets can be generated by setting two additional parameters: a shift $\gamma \in \mathbb{R}^d \times \mathbb{R}^{d'} / \mathcal{L}$ with $\gamma_\perp = \pi_\perp(\gamma)$, and a scale parameter $\lambda \in \mathbb{R}$. The projected set

$$\triangle_\gamma^\lambda(K) := \left\{x \in L \mid x^\star \in \lambda K + \gamma_\perp\right\} = \{\pi(y) \mid y \in \mathcal{L}, \pi_\perp(y) \in \lambda K + \gamma_\perp\}, \tag{2}$$

is called a model set. Note that we would have $\triangle_\gamma^\lambda(K) = \triangle_{\gamma'}^\lambda(K)$ if and only if $\gamma - \gamma' \in \mathcal{L}$.

Some properties are representative of model sets $\triangle$, which we review in Appendix A. Within a model set we can have different tiling configurations $\mathcal{T}_\triangle$ as reviewed in Appendix A.2. In this case, given an $x_i \in \triangle$ and a tiling $\mathcal{T}_\triangle$, one can associate to x_i different configurations of prototiles around it, called vertex types VT_i. A space-filling tiling will be given by a finite set of VTs. For completeness and to set the notation for the following presentation, we give a general outline in Appendix A for model sets and their associated patterns, tilings and symmetry.

Preprints (www.preprints.org) | NOT PEER-REVIEWED | Posted: 23 March 2022 doi:10.20944/preprints202111.0359.v2

Model sets and associated tilings don't retain discrete translational symmetry of the lattice in the embedding space, but they exhibit new discrete symmetries [38]. We will consider the scaling symmetry (self-similarity) associated to the scale parameter λ and the locally indistinguishable (LI) property associated to the shift parameter γ. Within a model set for some fixed γ a position x_i can be used as a fixed point, the similarity (or homothetic) center (κ), for a local inflation-deflation symmetry (LIDS) transformation (see A.3). A simple way to construct tilings with LIDS is by re-scaling the window by an appropriately scale parameter $\lambda \in \mathbb{R}$. Case by case we need to find a λ such that $\mathcal{T}_{\triangle(K)}$ and $\mathcal{T}_{\triangle(\lambda K)}$ are *mutually locally derivable*, $\mathcal{T}_{\triangle(K)} \overset{MLD}{\sim} \mathcal{T}_{\triangle(\lambda K)}$, which clearly can be inverted by re-scaling the window by λ^{-1}. We illustrate the procedure in Figure 1 for the one dimensional Fibonacci chain quasicrystals derived from the $\mathcal{L} = Z^2$ lattice. In this case the parallel space $\mathbb{R}^d$ is rotated from the Z^2 lattice vector by $\arctan(\phi^{-1})$, with scale parameter $\lambda = \phi$, where $\phi = \frac{\sqrt{5}+1}{2}$ is called the golden ratio. The set of parameters which give a good MLD equivalence class can be written as $\lambda^n = \lambda_o^n$ where λ_o, which works as a fundamental scaling ratio, is called an inflation multiplier. A simple geometric derivation of the inflation multiplier for the Fibonacci chain is given also in Figure 1. Note that when the window scales to a larger one than the original we call it a deflation (projected points become denser), and when the window scales to a smaller one we call an inflation (projected points become sparser).

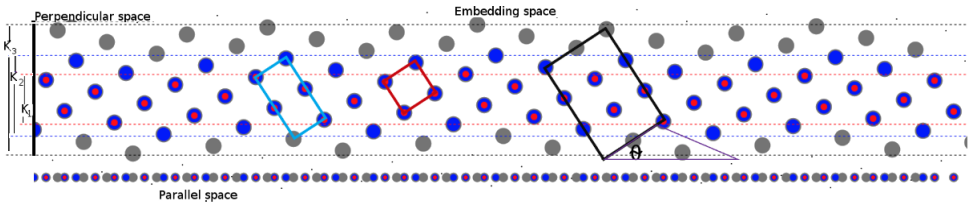

Figure 1. Three scaled Fibonacci chains in parallel space at the bottom generated by three scaled windows, K_1 in red, $K_2 = \phi K_1$ in blue and $K_3 = \phi^2 K_1$ in gray. The inflation multiplier is shown to be $\lambda_o = \phi$. The red window thickness is $\sin(\theta) + \cos(\theta)$. The blue first deflation window thickness is $\sin(\theta) + 2\cos(\theta)$. The black second deflation window thickness is $2\sin(\theta) + 3\cos(\theta)$ and the deflation at level n will have window thickness $Fib(n)\sin(\theta) + Fin(n+1)\cos(\theta)$, with Fib given the Fibonacci sequence. It can be checked that the ratio between the level n window thickness and level $(n-1)$ should be ϕ.

The relative frequency of VTs in some tiling $\mathcal{T}_{\lambda\gamma}$ of $\triangle_\gamma^\lambda$ ($VT^{\mathcal{T}_{\lambda\gamma}}$), given from Eq. (A1) in terms of ratios of window polytope volumes, is

$$f^r_{\triangle_\gamma^\lambda}(VT^{\mathcal{T}_{\lambda\gamma}}) = \frac{Vol(K_{VT^{\mathcal{T}_{\lambda\gamma}}})}{Vol(K_\gamma^\lambda)}, \tag{3}$$

where $K_{VT^{\mathcal{T}_{\lambda\gamma}}}$ is the window necessary to generate the cluster $VT^{\mathcal{T}_{\lambda\gamma}}$. $K_{VT^{\mathcal{T}_{\lambda\gamma}}}$ is contained in the window $K_\gamma^\lambda = \lambda K + \gamma$. This also applies to more general patterns in $\mathcal{T}_{\lambda\gamma}$, which can generate in most cases non-space-filling tilings (see Appendix A.2, Remark A2). To get the absolute frequency of the vertex type, $VT^{\mathcal{T}_{\lambda\gamma}}$, we take $dens(\triangle_\gamma^\lambda) f^r_{\triangle_\gamma^\lambda}(VT^{\mathcal{T}_{\lambda\gamma}})$. Note that the absolute frequency depends on the scale (l_g) of $\mathcal{G}$, but it is the same for tilings related by specific scale transformations generated by inflation multipliers λ_o, being an MLD invariant – it is invariant under LIDS.

Consider a general model set $\triangle_i = \triangle(K_i)$ where K_i can be $K_{\gamma_i}^{\lambda_i}$ or some other specification of K, such as a vertex type window $K_{VT^{\mathcal{T}^{\gamma\lambda}}}$. Then, given two model sets, $\triangle_i$ and $\triangle_j$, the overlap of their point sets we call *hits* $\triangle_{H_{ij}}$. Their window overlap is given by $K_{ij} = K_i \cap K_j$. The hits is then given by

$$\triangle_{H_{ij}} := \triangle(K_{ij}) = \left\{x \in (\triangle_i \cap \triangle_j)\right\} = \left\{\pi(y) \mid y \in \mathcal{L}, \pi_\perp(y) \in K_{ij}\right\}, \tag{4}$$

A measure of the global overlap of the model sets $\triangle_i$ and $\triangle_j$ inside one larger $\triangle_k$, $(\triangle_i \cup \triangle_j) \subset \triangle_k$ in the stack, is given in terms of their absolute frequency

$$H_{ij} = f^a_{\triangle_k}(\triangle_{H_{ij}}) = dens(\triangle_k)\frac{Vol(K_{ij})}{Vol(K_k)}. \tag{5}$$

Preprints (www.preprints.org) | NOT PEER-REVIEWED | Posted: 23 March 2022 doi:10.20944/preprints202111.0359.v2

3. Geometric State Sum Models from Model Sets, and Expectation Values

The object of interest here is analogous to the partition function in the context of statistical mechanics and thermodynamics, or the path integral in quantum mechanics. But in a discrete setting we move from integration to sums and, without a prior notion of Hamiltonian or Lagrangian (and associated Gibbs measures), we directly specify the weights or amplitudes. With a more general measure for the model set structures we will later discuss limits where one recovers measures with a usual Hamiltonian.

Usual state sums (see [30] for a recent review) aim to construct (quantum) invariants of a manifold from its triangulations or more general cell complex decompositions. The main point of those constructions is the state sum's independence of the choice of discretization. A physical application of state sums usually considered is as an intermediate tool between the path integral for a continuous theory in quantum gravity and a lattice approximation of the same theory. The basic idea that appears in many state sum constructions is to have a labeling scheme for some discretization, leading to a number which is shown to be an invariant, independent of the original discretization. In [31] we proposed the idea of labeling schemes for discrete models based on the discrete geometry of the discretization itself, which is straightforward to implement for general lattice-like models, in particular quasicrystals. At first glance, a labeling scheme based on the discretization itself seems to conflict with the desired goal of discretization independence, but this may be resolvable in structures that possess 'self' properties such as being self-modeling or self-contained. The tiling spaces of quasicrystals have such properties, so they are good candidates for this kind of scheme. If one chooses to model some system with some discrete mathematical structure, in particular in quantum gravity, the internal structure of the discrete system should provide the necessary elements for dynamics without need for additional external structures such as abstract labels or parameters – we call this geometric realism.

The tiling spaces associated to model sets are well understood, see [39] for a short review on the subject. Given a CPS $\mathcal{G}$ and a window K one has model sets $\triangle^{\lambda}_{\gamma}$ and tilings $\mathcal{T}_{\lambda\gamma}$. Then a specific tiling $\mathcal{T}_{\lambda\gamma}$ is a point in the associated tiling space $X_{\lambda\gamma}$ of the given CPS. By varying γ one can get more model sets and associated tilings, which are new points on this space. The tiling space is in general very complicated but it will have nice properties, such as compactness, if the tilings have nice properties, such as those presented in Appendix A.2 (discussed there for model sets with the name of geometric hull, which can be continuous or discrete). Such are the tilings under consideration here, where we will focus more on the tilings' properties rather than the full space properties. So a point on the $X_{\lambda\gamma}$ space has internal structure given by the model sets and associated tilings' discrete structures, allowing for the notion of geometric realism. A natural invariance on this space is the LIDS. Given a point or tiling $\mathcal{T}_{\lambda\gamma}$ of $\triangle^{\lambda}_{\gamma}$, there is a finite number of VTs where their relative frequencies $f^{r}_{\triangle^{\lambda}_{\gamma}}(VT^{\mathcal{T}_{\lambda\gamma}})$, Eq. (3), are invariant under transformation to a new tiling $\mathcal{T}_{\lambda'\gamma}$ with $\mathcal{T}_{\lambda\gamma} \overset{MLD}{\sim} \mathcal{T}_{\lambda'\gamma}$ (the mutually locally derivable relation $\overset{MLD}{\sim}$ is explained in Appendix A.2).

Another object that retains LIDS invariance (under re-scaling in parallel space, which we will discuss later) is the hits measure, Eq. (5). The relative frequencies and hits measure will be our main building blocks in the construction of the probabilistic measure below. Given a tiling space $X_{\lambda\gamma}$ for a given $\mathcal{G}$ and window K, we focus on one point in this space, which represents one of many specific tiling configurations. We can then construct a partition function or state sum model for the internal structure of this point. To specify the configuration of states and associated weights we also consider some general principles:

1- *Superposition*: Given a finite set (from a finite number of translations of the shift γ) of different tiling configurations (space-filling or not) $\mathcal{T}^{\gamma}_{\triangle} \subset \mathcal{T}_{\triangle}$, with $\mathcal{T}_{\triangle} = \{\mathcal{T}_{\lambda\gamma}\}$ for fixed λ, there are weights $W_{\mathcal{T}^{\gamma}_{\triangle}}$ associated with them and we consider the dynamic state sum

$$W_{\mathcal{T}_{\triangle}} = \sum_{\mathcal{T}^{\gamma}_{\triangle} \subset \mathcal{T}_{\triangle}} W_{\mathcal{T}^{\gamma}_{\triangle}}. \tag{6}$$

Preprints (www.preprints.org) | NOT PEER-REVIEWED | Posted: 23 March 2022 doi:10.20944/preprints202111.0359.v2

2- *Locality*: Weight mainly encodes local information. Tilings allow global regularity to result from the structure of local configurations

$$W_{\mathcal{T}^{\gamma}_{\Delta}} = \prod_{VT_{ij} \sqsubset \mathcal{T}^{\gamma}_{\Delta}} W_{VT_{ij}}, \tag{7}$$

where the pair of vertex types (ij) provides information on the connectivity of space-filling tilings, and in the case of non-space-filling tilings we consider a ball of radius R (as in Appendix A, Remark A1) with respect to the subset $\mathcal{T}^{\gamma}_{\Delta}$. The symbol $\sqsubset$ means that the vertex type is a valid fragment of the tiling $\mathcal{T}^{\gamma}_{\Delta}$.

3- *Geometric realism*: The symmetry of the local weights should reflect the symmetry of the underlying discrete geometry as discussed above (see also [31,40]). Implementing the symmetry at the level of the weight itself has the bonus that the implementation of superposition of local configurations by the imposition of the first principle above must take into account the admissible geometric configurations of the tiling configuration space. A signature of the local configuration is given by the relative frequency of the local VT and its hits interactions with neighbors, Eq. (5), with $\Delta_k = \Delta^{\lambda}_{\gamma}$, $K_i = K_{VT_i^{\mathcal{T}^{\gamma\lambda}}}$, $K_j = K_{VT_j^{\mathcal{T}^{\gamma\lambda}}}$ and $K_k = K^{\lambda}_{\gamma}$, which we denote by $H^{\lambda}_{ij} = dens(\Delta^{\lambda}_{\gamma})\frac{Vol(K_{ij})}{Vol(K^{\lambda}_{\gamma})}$. This leads to the definition of the local weights,

$$W_{VT_{ij}} = F[f^{r}_{\Delta^{\lambda}_{\gamma}}(VT^{i}) f^{r}_{\Delta^{\lambda}_{\gamma}}(VT^{j}) H^{\lambda}_{ij}], \tag{8}$$

where the function F, which could give the usual Boltzmann weights, here will be taken as

$$F[f] = \begin{cases} 1, & f = 0, \\ f, & otherwise, \end{cases} \tag{9}$$

Theorem 1 (Geometric State Sum LIDS Invariance)**.** *For a given CPS with model sets of fixed density, the state sum $W_{\mathcal{T}_{\Delta}}$ is invariant under LIDS transformation $\mathcal{T}^{\gamma\lambda}_{\Delta} \to \mathcal{T}^{\gamma\lambda'}_{\Delta}$ with $\mathcal{T}^{\gamma\lambda}_{\Delta} \overset{MLD}{\sim} \mathcal{T}^{\gamma\lambda'}_{\Delta}$.*

PROOF. The frequencies Eq. (3) are ratios of volumes, which are scaled by the same inflation parameter $\lambda^n = \lambda'/\lambda$, so that they are invariant under LIDS. The hits overlap with all neighbors can also be quantified by the polytope overlap of their windows, which means it defines a locally finite specific cluster C_{ij} with window $K_{C_{ij}}$ such that hits reduces to the relative frequency of C_{ij} multiplied by the density of Δ. The density, Eq. (A3), remains constant if we re-scale the parallel space by the same inflation multiplier. Due to the properties of locally finite structure and finite local complexity, Remark A1, $W_{\mathcal{T}^{\kappa}_{\Delta^n}}$ can always be written as a product of a finite number of the relative frequencies of clusters C_i with windows K_{C_i}, where these clusters include the VTs and the ones generated by the hits (C_{ij}). But in the larger $\mathcal{N}$ limit, the number of a specific cluster C_i in the general product over a tiling must approach its frequency, so that we can write $W_{\mathcal{T}^{\gamma}_{\Delta}} = \prod_i^{n'} \left(f^{r}_{\Delta^{\lambda}_{\gamma}}(C_i) \right)^{f^{r}_{\Delta^{\lambda}_{\gamma}}(C_i)\mathcal{N}}$, with n' the number of clusters (C_is). As the relative frequencies are invariants, $W_{\mathcal{T}^{\gamma}_{\Delta}}$ is invariant.

This means that $W_{\mathcal{T}_{\Delta}}$ is a sum over the LIDS invariants, and by fixing λ it counts just one element of each LIDS MLD equivalence class. We note that there are two scales involved, one being the inflation scale fixed by λ and another the scale l_g for the CPS $\mathcal{G}$, which sets the scale in parallel space. Including the scale l_g maintains the invariance at each fixed l_g. So we assume that in $W_{\mathcal{T}_{\Delta}}$, Δ has encoded the scale l_g.

A probability measure on the finite tiling space is given from

$$\mu_{\mathcal{T}^{\gamma}_{\Delta}}(\mathcal{T}^{\gamma}_{\Delta}) = \frac{1}{W_{\mathcal{T}_{\Delta}}} W_{\mathcal{T}^{\gamma}_{\Delta}}, \tag{10}$$

Preprints (www.preprints.org) | NOT PEER-REVIEWED | Posted: 23 March 2022 doi:10.20944/preprints202111.0359.v2

and the expectation value of a measurable function $f : \mathcal{T}^{\gamma} \to \mathbb{R}$ by

$$E_{\triangle}[f] \coloneqq \mu_{\mathcal{T}^{\gamma}_{\triangle}}(f) = \sum_{\mathcal{T}^{\gamma}_{\triangle} \subset \mathcal{T}_{\triangle}} f(\mathcal{T}^{\gamma}_{\triangle}) \frac{1}{W_{\mathcal{T}_{\triangle}}} W_{\mathcal{T}^{\gamma}_{\triangle}} \tag{11}$$

3.1. Dynamics—Computational Aspects of Tiling Spaces

The state sum and probabilistic measure constructed above aim to describe one point in the tiling space. To describe dynamics on the tiling space, such as the transition $W_{\mathcal{T}_{\triangle}}(x_i) \to W_{\mathcal{T}_{\triangle}}(x_j)$, with x_i, x_j being points of the tiling space $X_{\lambda\gamma}$, one would need to study its topology and attach a metric in this space. Here we will avoid that by continuing to focus on the tiling properties themselves.

The probabilistic measure built above allows us to define random walks on $X_{\lambda\gamma}$. Basically, if we sample a path on $X_{\lambda\gamma}$ with N points, t^l ($l = 1, ..., N$), between x_i and x_j, each point in this path corresponds to one tiling from the sum Eq. (6) with a certain probability. We can restrict the set of tilings in the tiling space, and thus in each path, by considering that the initial tiling at x_i have a specific VT at the origin (let us call it κ_i) and requiring that the tilings in the path t^l and in x_j are in the $\mathbb{Z}$-module of κ_i, $Z(\mathcal{T}^{\kappa_i}_{\triangle})$, Eq. (A9). Then each point in the path can have a tiling from a subset of γ translations that is in $Z(\mathcal{T}^{\kappa_i}_{\triangle})$, $\mathcal{T}^{\kappa_i}_{\triangle} \subset \mathcal{T}_{\triangle}$. Associated to this path there is a ordered set of tiling configurations (an assignment of a tiling for each point), which we call an *animation* $A_{t_{\kappa_i}}$

$$A_t^{c_{\kappa_i}} = \left\{ \mathcal{T}^{\kappa_i}_{\triangle_{t^l}} \mid l = 1...N \right\}, \tag{12}$$

with cardinality N and c_{κ_i} representing a specific set of tilings that are translations of κ_i. By repeating this procedure M times we generate a set of animations $A_t^{\kappa_i} = \left\{ A_t^{c_{\kappa_i}} \mid c_{\kappa_i} = 1...M \right\}$.

Now we are in position to state a fourth constraining principle, for the state sums under consideration, to deal with dynamics in the tiling space.

4- *Principle of efficient language* (PEL) [41–43]: This aims to implement a notion of efficiency in discrete or computational systems, which are codes or languages. The random walks with their associated animation sets $A_t^{\kappa_i}$ above can be interpreted as a form of look-ahead algorithm (so-called look-savings-ahead algorithm in [31]) that allows us to define two *computational functions* that can be coupled to the geometric state sum model. First we consider the so-called *hit potential*, Y, which takes values on the natural numbers including zero, $Y : \mathcal{T}^{\lambda}_{\triangle} \to \mathbb{N}$. We start with the initial condition of a tiling at x_i with κ_i at the origin, which generates the subset of translations $\mathcal{T}^{\kappa_i}_{\triangle} \subset \mathcal{T}_{\triangle}$ from which each point of one animation will be sampled. So at the initial tiling for each $\kappa_j = VT^j$ position, which is a valid position for κ_i, the hit potential Y_j can be defined by the number of tilings on the full set of animations that uses that position κ_j

$$Y_j = card\left(\left\{ \mathcal{T}^{\kappa_i}_{\triangle_t} \subset (\cup A_t^{c_{\kappa_i}}) \mid \kappa_j \sqsubset \mathcal{T}^{\kappa_i}_{\triangle_t} \right\} \right). \tag{13}$$

The second function considered is the called *savings potential*, $S : \mathcal{T}^{k} \to \mathbb{N}$. In each animation $A_t^{c_{\kappa_i}}$ we count the number of vertex type κ_i overlaps in the union of all tilings steps

$$S\left(A_t^{c_{\kappa_i}}\right) = card\left(\left\{ \kappa_i \sqcap (\mathcal{T}^{\kappa_i}_{\triangle_{t^l}} \subset A_t^{c_{\kappa_i}}), l = 1, ..., N \right\} \right). \tag{14}$$

In this way we can consider transitions on the tiling space

$$W_{\mathcal{T}_{\triangle}}(x_j) = W_{\mathcal{T}^{\gamma}_{\triangle}}(x_i) W_{A_t^{\kappa_i}}, \tag{15}$$

with

$$W_{A_t^{\kappa_i}} = \sum_{A_t^{c_{\kappa_i}} \subset A_t^{\kappa_i}} S\left(A_t^{c_{\kappa_i}}\right) \sum_{\mathcal{T}^{k} \subset A_t^{c_{\kappa_i}}} W_{\mathcal{T}^{k}}, \tag{16}$$

Preprints (www.preprints.org) | NOT PEER-REVIEWED | Posted: 23 March 2022 doi:10.20944/preprints202111.0359.v2

and a new state sum can be defined for transitions

$$W_{\mathcal{T}_\Delta}(x_j) = \sum_{\mathcal{T}_\Delta^\gamma \subset \mathcal{T}_\Delta} W_{\mathcal{T}_\Delta^\gamma}(x_i) W_{A_t^{\kappa_i}}, \tag{17}$$

with $W_{VT_{ij}} = F[f^r_{\Delta^\lambda_\gamma}(VT_i) f^r_{\Delta^\lambda_\gamma}(VT_j) H^\lambda_{ij} Y_i Y_j]$ in $W_{\mathcal{T}_\Delta^\gamma}$.

Now a recursive look-savings-ahead algorithm can be designed to implement dynamics such that the use of computational resources are minimized. For example one can generate one initial set of animations from some initial tiling. Then a second set of animations can be generated by using the first animations to compute the hit and savings potentials, changing the probabilistic measure through Eq. (17), and so on. The algorithms can be exploited to generate dynamics which maximize the savings potential, which allow for minimizing the resources for handling the large set of animations, while at the same time favoring local connectivity through the hit potential.

A last point in this section is the possibility to define expectation values. One natural expectation value of interest is for the tiling state itself, $W_{\mathcal{T}_\Delta^\gamma}$,

$$E_\Delta[W_{\mathcal{T}_\Delta^\gamma}] = \frac{1}{W_{\mathcal{T}_\Delta}} \sum_{W_{\mathcal{T}_\Delta^\gamma} \sqsubset W_{\mathcal{T}_\Delta}} W^2_{\mathcal{T}_\Delta^\gamma} W_{\mathcal{T}^\gamma_{A_{\kappa_i}}}. \tag{18}$$

Another expectation value that can be considered is one for the autocorrelation function Eq. (A4),

$$E_\Delta[\gamma_\Delta] = \frac{1}{W_{\mathcal{T}_\Delta}} \sum_{\mathcal{T}_\Delta^\gamma \subset \mathcal{T}_\Delta} \gamma^{\kappa_i}_\Delta W_{\mathcal{T}_\Delta^\gamma} W_{A_t^{\kappa_i}}, \tag{19}$$

$$\tag{20}$$

where $\gamma^{\kappa_i}_\Delta$ is the autocorrelation on the inital tilings with regards to the translations of κ_i. This expectation value allows one to define an order parameter, called the hit average $\overline{H}$,

$$\overline{H}_\Delta = \frac{E_\Delta[\gamma_\Delta]}{N}. \tag{21}$$

3.2. Model Set Examples

The model sets of interest here are the ones for $d = 3$. The most studied family of model sets are those for which the relative frequency, Eq. (A1), of their VTs are elements of the ring of integers [15], here called Dirichlet integers,

$$\mathbb{Z}[\phi] = \{m + n\phi \,|\, m, n \in \mathbb{Z}\}, \tag{22}$$

where ϕ is again the golden ratio. This family includes the 3-dimensional icosahedral model sets [15]. The two main examples are projected from the Z^6 lattice, $\mathcal{G}_{Z^6} = (\mathbb{R}^3, \mathbb{R}^3, Z^6)$, and from the D_6 lattice, $\mathcal{G}_{D_6} = (\mathbb{R}^3, \mathbb{R}^3, D_6)$. The $\mathcal{G}_{Z^6}$ model set has 24 VTs and $\mathcal{G}_{D_6}$ has 36 VTs, and tables with explicit values for the relative frequencies can be found for example in [44].

For these two model sets the scale invariant part—basically, cluster frequencies—of the state sums, probabilistic measures and expectation values defined in the previous section, are elements of $\mathbb{Z}[\phi]$, as its powers are again in $\mathbb{Z}[\phi]$ due to $\phi^2 = \phi + 1$.

The $\mathcal{G}_{Z^6}$ and $\mathcal{G}_{D_6}$ model sets give space-filling tilings. Possible λ^n-inflation non-space-filling tilings in these cases can be re-scaled to space-filling ones. Their VTs are not regular polytopes, but are deformed projections from groups of hyper-dimensional regular polytopes in the embedding lattice. Other examples are derived from the E_8 lattice [45], which are non-space-filling tilings, so-called compound quasicrystals (CQC) or n-component model sets (see [15] for an example of a 3-component model set describing the Danzer's ABCK tiling). E_8 has a well known 4-dimensional model set implementation, the so-called Elser-Sloane model set [46], which can be naturally extended to 3-dimensional model sets [21]. The 3-dimensional E_8-CQC uses a different approach by considering 6-dimensional sub-spaces of E_8. $\mathcal{G}^n_{E_8} = (\mathbb{R}^3, \mathbb{R}^3, L^6_n \subset E_8)$. One can employ the

Preprints (www.preprints.org) | NOT PEER-REVIEWED | Posted: 23 March 2022 doi:10.20944/preprints202111.0359.v2

usual CPS on the 6-dimensional sub-spaces by considering the canonical window from the Voronoi polytope there, but as we don't need space-filling tilings, the spherical approximation here can be taken as the window defining the CPS. The construction relies only on one window K and λ^n-inflations given by powers of ϕ. This construction makes it possible to combine periodic and aperiodic order by having model sets with tilings with regular VTs, which are tetrahedrons or groups of tetrahedrons, where the groups considered are multiples of groups of four tetrahedrons, up to 20 ($n4G$, $n = 1, 2, 3, 4, 5$), that can occupy the same center position κ_i and generate convex hulls of crystallographic objects such as the cuboctahedron.

This procedure gives the relative frequencies for λ^n-inflation tilings to be elements of $\mathbb{Z}[\phi^{-1}]$, and to be the same for all $n4G$s. The relative frequencies are therefore the same for the different $n4G$s, and the important part is the scale dependent density $dens(\triangle_{n4G})$.

In the next section we provide a novel method for constructing the E_8-CQCs, the so-called *texture model set scheme* (TMS), to do the explicit computations by embedding in a particular lattice, a set which is isomorphic and very close to the original model set.

3.2.1. Explicit construction of the E_8-CQC

An analytical method to build the $Z[\phi]$-related model sets and the CQCs, which gives analytical foundations for the densities and vertex type frequencies, has been recently developed. We'll describe the analytic construction of a model set, in lattice coordinates, with a lattice of the target space, not of the embedding space. This makes for a huge dimension reduction and accelerates the computation, without any loss of information of the model set.

The union of five model sets of $\mathcal{G}^n_{E^8}$, compounded together in a unique 3-dimensional space embedded in $\mathbb{R}^3$, is a discrete set in $\mathbb{D}^3$, the cartesian product of 3 instances of the so-called Dirichlet ring, see equation (22). Our new description of this model set considers a discrete texture of the target space embedded in a lattice ($\mathbb{Z}^3$ in 3-dimensions), and a family of coordinate transformations between the most compact set and the exact model set in $\mathbb{D}$ coordinates.

Using the same notation of section 2 we define a TMS as a 3-tuple $\mathcal{G}' = \left(\mathbb{Z}^d, G', \mathcal{L}\right)$, where $\mathbb{Z}^d$ is a euclidean cubic lattice, G' is a bounded region, the image of a unit cube under a nonlinear transformation of $\mathbb{Z}^d$, and $\mathcal{L}$ is a lattice in $\mathbb{Z}^d \times G'$, with the two natural projections π:$\mathbb{Z}^d \times G' \to \mathbb{Z}^d$ and $\pi_\perp$:$\mathbb{Z}^d \times G' \to G'$. With $L = \pi(\mathcal{L})$, π is a bijection between $\mathcal{L}$ and L, and $\pi_\perp(\mathcal{L})$ is dense in G'. $\mathcal{E} = \mathbb{Z}^d \times G'$ is again the embedding space, the space $\mathbb{Z}^d$ is the parallel space and G' is the *virtual perpendicular* or *virtual internal space*.

This scheme has also the well-defined star map applied to G', $\star : L \to G'$:

$$\star(x) = x/\phi - \lfloor x/\phi \rceil. \tag{23}$$

The star cube $\star(\mathbb{Z}^3)$ is a cube of unit edge length, centered at point $O = \{0, 0, 0\}$. The virtual spherical cut window is inside of this cube but has a smaller diameter ϕ^{-1} and is centered on κ_i. Restricting to points that are centroids of a specific VT corresponds to operating on a subset of the star cube. For the VT of a group of 4 tetrahedrons, whose convex hull is a cuboctahedron, the restriction in the star cube is simply a smaller O-centred star cube of diameter $3\phi^{-7}$. We'll define in Appendix B a function $f_V(k)$ such that all model set vertices are in $f_V(\mathbb{Z})^3$ and $2|f(\mathbb{Z})| < \phi^{-1}$, and a function $f_{4G}(k)$ such that all 4G-centroids are in $f_{4G}(\mathbb{Z})^3$ and $2|f_{4G}(\mathbb{Z})| < 3\phi^{-7}$.

More details on the CQC implementation, such as how to get the precise coordinates, are shown in Appendix B.

The relative frequencies for tilings are computed from the distance in the perpendicular space between the star maps of two similarity centers, κ_i and κ_j, whose square is a Dirichlet integer.

$$d^2(\star(\kappa_i), \star(\kappa_j)) = (\overrightarrow{\star(\kappa_i)} - \overrightarrow{\star(\kappa_j)})^2 \tag{24}$$

The relative volume of the intersection of two balls of radius 1, whose centers are distant by d, with respect to the enclosing ball of radius ϕ is (see Eq. 5)

$$\frac{Vol(K_{\kappa_{ij}})}{Vol(K)} = \frac{1}{16\phi^3}(2-d)^2(4+d). \tag{25}$$

Preprints (www.preprints.org) | NOT PEER-REVIEWED | Posted: 23 March 2022 doi:10.20944/preprints202111.0359.v2

If $d = m + n\phi$ the powers of ϕ here can be reduced to give

$$\frac{Vol(K_{\kappa_{ij}})}{Vol(K)} = (2\phi - 3) + \frac{3}{4}((3m - 2n) + \phi(-2m + n)) + \frac{1}{16}((-3m^3 + 6m^2n - 3mn^2 + n^3) + \phi m(2m^2 - 3mn + 3n^2)). \quad (26)$$

When $i = j$ we have the relative frequency of the inflation window given by $(2\phi - 3) = \phi^{-3}$, which is the volume of a ball of radius one relative to a ball of radius ϕ. For $|d| < 2/\phi$, $\frac{Vol(K_{\kappa_{ij}})}{Vol(K)} < \phi^{-3}(1 - 2\phi d/5)$ which is a good linear approximation.

4. Implications

In physical terms, the quasicrystal structures described by the higher dimensional model set mathematics discussed here are positioned at large scales or low energy, such as the quasicrystal materials built upon fundamental particles over the geometry of spacetime. The agreement of the model set theory with experiments involving quasicrystal materials is remarkable as we discussed in the introduction. Here we'll discuss implications to push the model set structures to short distances, such as the Planck scale, as a candidate for the unification structure for quantum gravity and particle physics.

The approach of entropic or emergent gravity [1,2] considers a particle of mass m approaching a holographic screen from the side where spacetime has already emerged. The holographic principle is applied to assume the encoding of the microscopic configurations behind the screen, N_c, in the area A_s of the screen, $N_c \propto A_s$. Then the law of inertia, the equivalence principle, Newton's gravitational law, or Einstein equations can be derived. In this paradigm, gravity is an entropic force emergent from the underlying configuration of quantum matter. One thus transfers the problem of emergence of spacetime to the problem of emergence of quantum matter. Once one has mass and energy distributions and their dynamics, gravity will emerge. Essentially, the holographic principle and the associated covariant entropy bound are linked to regimes where spacetime can be classically well approximated with sufficient matter content. Nevertheless, the linking of the bound to the area and not to the volume of the region gives strong evidence in favor of unitarity of the underlying quantum field theory rather than locality of quantum fields, because quantum evolution preserves information. It is noteworthy that the locality principle in section 3 refers to the state sum weights of the tiling space structures, which is about the local topology given from those structures. We will require in the construction below emergent quantum evolution unitarity without need to refer to emergent locality in a relational description.

So, how does one define evolution without a prior notion of spacetime, regarding gravity as the geometry of spacetime? The problem is finding a unification of general relativity with quantum mechanics in a theory of quantum gravity, usually referred to as the problem of time in quantum gravity [33–36]. One approach, called internal time, is to consider relational evolution where some physical degree of freedom evolves relative to others, with the dynamics governed by more general Hamiltonian constraints [47]. This works well if the degree of freedom playing the role of internal time behaves monotonically, which is generally not the case. The physical system's internal time can be a quantum field, such as a scalar field in cosmology, or some underlying structure. In general, the choice of internal time or clocks is local and dynamic, which is the same problem as gauge fixing in the quantization of gauge theories [37,48,49]. This leads to the conclusion that the problem of time is a special case of the so-called Gribov problem in general gauge theories. In other words, how does one define global evolution with respect to some underlying oscillating clock system with turning points? One simple model system solution was given recently [37], where one distinguishes three necessary notions of time, the usual background time parameter, the global monotonic relativistic one and a new notion of a clock variable. One of the implications of having the model set tiling spaces as the underlying structure is that it can play the role of the underlying clock, providing the global monotonic time and the clock variable for relativistic unitary quantum evolution.

Preprints (www.preprints.org) | NOT PEER-REVIEWED | Posted: 23 March 2022 doi:10.20944/preprints202111.0359.v2

4.1. An Ergodic Correspondence: Internal Mass, Clock and Inertia

In usual model sets relative frequencies are uniformly distributed, so one expects to have ergodicity [15,29], but here the savings and the hit potentials allow for dynamics that steer probabilities away from uniform distributions. Another feature that can lead away from ergodicity is the more general possibility of less homogeneous non-space-filling tilings. A further aspect is that we don't want to use the model set framework to model fundamental particles here; rather, we want to maintain the usual description at the particle scale, but make it compatible with a hypothetical model set tiling space structure at a smaller (perhaps Planck-level) scale. So let us say we have a quantum system in the usual equilibrium situation with a valid measure given by a usual path integral measure [32], μ_{PI}, implementing physics laws such as momentum and energy conservation. Now if this system has an underlying structure given by $\mu_{\mathcal{T}^\lambda_\triangle}$ and we have some expectation value of some function computed with the $\mu_{PI}(f)$ measure, we can stipulate a correspondence with $\mu_{\mathcal{T}^\lambda_\triangle}(f)$ by identifying a good regime where the correspondence could apply. This leads us to propose the following function,

$$f^h_\triangle[f] = \delta(\mu_{\mathcal{T}^\lambda_\triangle}(f) - \mu_{PI}(f)), \tag{27}$$

which aims to connect different ensemble and time averaging measures. If we locate the quantum system in atomic or sub-atomic scales and the tiling spaces at the Planck scale we can coarse grain the tiling space to infer intrinsic properties of the quantum system. The function Eq. (27) allows us to establish a correspondence between quantities in both probabilistic measures. Due to Theorem 1, frequencies of clusters in one point (tiling) of a tiling space are natural conserved quantities under re-scaling to be mapped to physical quantities such as mass and energy.

According to Theorem 1, the limit that is of interest for the point averaging of tiling space $X_{\lambda\gamma}$ is taking a large number of tiles, N. This can be implemented for a fixed λ^n by just extending the parallel space to a larger and larger size for each different γ tiling, which entails projecting more and more points from the embedding lattice, with a corresponding higher density in the window in the perpendicular space. Now, coarse graining can be achieved by scaling the window for specific values of λ, which preserves LIDS, $\lambda^n = \lambda^n_o$, with an inflation multiplier λ_o. For the Fibonacci chain and the examples of section 3.2 we can set the inflation multiplayer to be $\lambda_o = \phi^{-1}$. In this large N regime the state sum works as a partition function, which, from the proof of Theorem 1, reduces to a product of cluster frequencies $\prod_i^{n'} f_i^{f_i N}$. Asymptotically this has the exponential expression $e^{N(\lambda^n)(\sum_i f_i ln(f_i))}$, where the number of tiles grows with the number of inflations of the window. The new quantity that appears in the exponential we identify with the information entropy of the tiling state,

$$I_{\mathcal{T}_k} = -\sum_i f_i ln(f_i). \tag{28}$$

In terms of the partition functions we can re-state the proposed correspondence from Eq. (27) as

$$\sum_{\mathcal{T}^\gamma} e^{-N(\lambda^n) I_{\mathcal{T}^\gamma}} - \sum_i e^{-\beta E_i} = 0 \tag{29}$$

which allows us to establish a correspondence between tiling state probabilities and large scale (emergent) energy state probabilities, with $N(\lambda^n)$ corresponding to inverse temperature, and cluster frequencies (or their information entropy) corresponding to energy.

Consideration of explicit hadronic states [50] with $E_{nl} \sim M_h^{\frac{3}{2}}(2n + l - \frac{1}{2})^{\frac{2}{3}}$ gives a direct map of hadronic masses M_h and $I_{\mathcal{T}^\gamma}$. Interestingly, for a given tiling space the values $I_{\mathcal{T}^\gamma}$ are bounded from above. This is easily seen for Eq. (28), where ignoring hits reduces the VT frequencies, which we compute for $\mathcal{G}_{\mathbb{Z}^6}$ as shown in Figure 2. Including hits, they are ratios of volumes of associated clusters' windows over a fixed larger window. Using the spherical approximation for the windows and considering that for the model sets of interest the radius is a number in $\mathbb{Z}[\phi^{-1}]$ or $\mathbb{Z}[\phi]$ such that the radius can be written as $(m + n\phi^p)$ where $m, n \in \mathbb{N}$ and $p \in \mathbb{Z}$, allows us to get $I_{\mathcal{T}^\gamma}$ from Eq. (28). The general form of Eq. (28) is invariant over the variations of the parameters and is shown in Figure 3 where, without normalization, it has a maximum of Euler's number, e^{-1}, but with most states being on lower scales away from this maximum, and with visible gaps. An expanded view of a smaller range is shown in Figure 4.

Preprints (www.preprints.org) | NOT PEER-REVIEWED | Posted: 23 March 2022 doi:10.20944/preprints202111.0359.v2

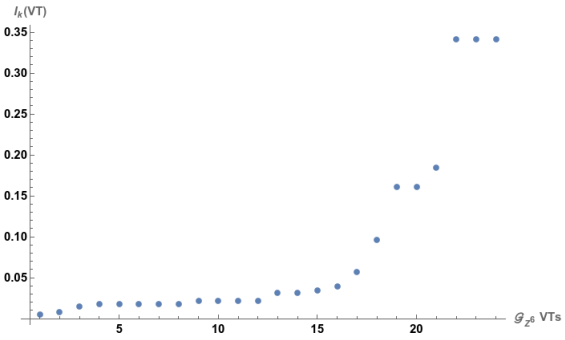

Figure 2. I_k for each of the 24 VTs of $\mathcal{G}_{Z^6}$.

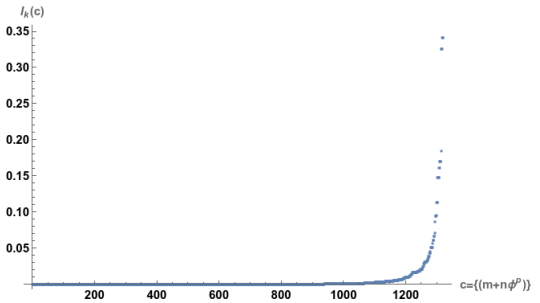

Figure 3. Sorted I_k for different windows with radius $(m + n\phi^p)$ in a large window $(m_{max} + n_{max}\phi^{p_{max}})$.

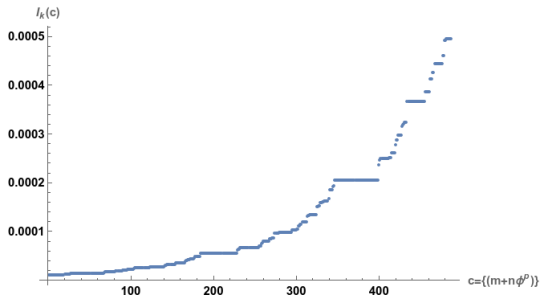

Figure 4. Expanded view at an intermediary scale of sorted I_k for different windows with radius $(m + n\phi^p)$ in a large window $(m_{max} + n_{max}\phi^{p_{max}})$.

So far we have been concerned with one point on a tiling space and intrinsic properties of large scale quantum systems. Fixing a CPS and a window K fixes the possible clusters' relative frequencies and associated information entropy, and hence a possible spectrum, such as the one in Figure 3. To illustrate how a CPS could be used through the ergodic correspondence to predict the hadronic spectrum we show a plot of the hadron masses (with the large mass normalized to e^{-1}) in Figure 5 and include the known fundamental particles such as quarks and the massive bosons in Figure 6. Similar features to Figure 3, such as gaps, a bound on higher mass states and a dense distribution from below can be noted, which motivates more research in this direction.

The fact that the energies E_i come from the Hamiltonian of the system suggests that we can state this correspondence in terms of a Hamiltonian constraint $\delta(H_{\mathcal{T}} - H)$, with H a Hamiltonian for the system and $H_{\mathcal{T}}$ providing new variables for relational evolution from the internal averaging over tiling space.

Consider now a specific large scale system with a canonical pair of degrees of freedom (q, p) and some Hamiltonian $H(p, q)$. We propose to extend the large and small (internal) correspondence to the transitions in tiling space Eq. (15) or the new non-ergodic state sum Eq. (17). In this way a transition in the canonical conjugate pair (q, p) from H should be accompanied by a suitable new pair of variables coming from expectation values from the underlying tiling space with a suitable emergent Hamiltonian $H_{\mathcal{T}}$. Now we want to synchronize transitions from an initial state q_i to a final state q_j, $q_i \to q_j$, with the transition between two points x_i and x_j in the internal tiling space $X_{\lambda\gamma}$.

Preprints (www.preprints.org) | NOT PEER-REVIEWED | Posted: 23 March 2022 doi:10.20944/preprints202111.0359.v2

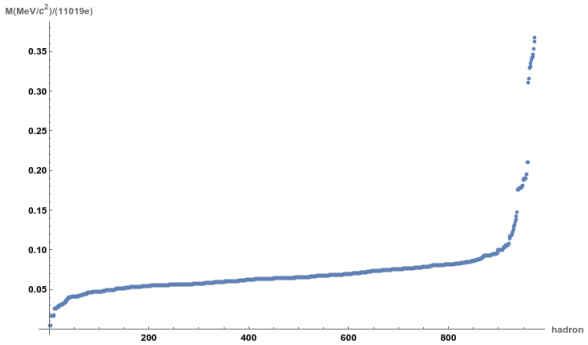

Figure 5. Hadronic masses M in MeV/c^2 normalized by the largest mass going to e^{-1}. We used the ParticleData function from the Mathematica software.

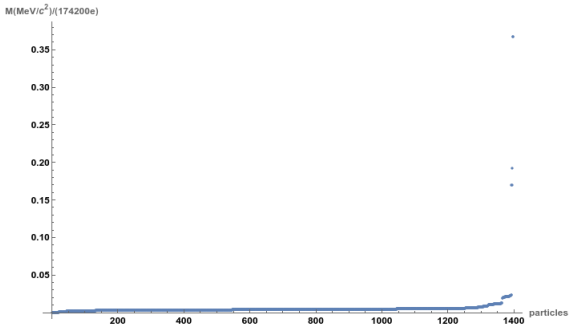

Figure 6. Hadronic and other fundamental particles masses M in MeV/c^2 normalized by the bigger mass going to e^{-1}. We used the ParticleData function from the Mathematica software.

We re-state the correspondence Eq. (27) for the Hamiltonians $H_{\mathcal{T}}$ and H as $\delta(H_{\mathcal{T}} - H)$, suggesting the emergence of Hamiltonian constraints (C) for this kind of dynamics, $C = H_{\mathcal{T}} - H = 0$. To specify a pair of of degrees of freedom for $H_{\mathcal{T}}$, we consider, as in section 3.1, that the tilings in the steps $x_i \to x_j$ are sampled from a subset, which are translations of the initial tiling at x_i, with a specific vertex type κ_i at the origin. Note that a specific vertex type has some specific relative frequency in a given CPS with window K, and so a specific I_k corresponding to a specific rest mass. When sampling a path with Eq. (17), the natural variable to parameterize a path in tiling space is the possible translations t of κ_i, in the parallel space of the CPS. Position in the parallel space has a natural conjugate variable, which is the projection of the dual lattice to parallel space, and which arises on the Fourier domain of functions in parallel space. See the variable $k \in \overline{L} = \pi(\overline{\mathcal{L}})$, $\overline{\mathcal{L}}$ the dual lattice of $\mathcal{L}$, in Eq. (A5) and Eq. (A6). So we have a natural pair of effective degrees of freedom, which is the translation in parallel space t and its dual, from a Fourier transform, here called p_t, (t, p_t). This permits a more explicit expression for the Hamiltonian constraint, which in the relativistic case will be given by $C = H^2_{\mathcal{T}}(t, p_t) - H^2(q.p) = 0$ (for example $C = p^2 + m^2 - p_t^2 - t$ or $C = p^2 + m^2 - p_t^2 - t^2$). This kind of system leads to an action principle

$$S = \int_{\tau_i}^{\tau_j} d\tau (p\dot{q} + p_t\dot{t} - NC), \tag{30}$$

where N is an auxiliary variable whereby the variation imposes the constraint $C = 0$. Then relational evolution can be employed by a gauge fixing $t = f(\tau)$, which selects t as the internal time variable [37] leading to the associated transition amplitudes given by

$$(q_i t_i \tau_i | q_j t_j \tau_j) = \int D_m \exp\left(\frac{i}{\hbar} \int_{\tau_i}^{\tau_j} d\tau (p\dot{q} + p_t\dot{t} - NC)\right), \tag{31}$$

with D_m an appropriate path-integral measure, and paths restricted so that $q(\tau_i) = q_i$, $q(\tau_j) = q_j$, $t(f(\tau_i)) = t_i$ and $t(f(\tau_j)) = t_j$. The new time variable t depends on the underlying dynamics of transitions on tiling space, and if it has good monotonic behaviour with respect to τ, unitary

Preprints (www.preprints.org) | NOT PEER-REVIEWED | Posted: 23 March 2022 doi:10.20944/preprints202111.0359.v2

evolution is straightforward. Even if it is an oscillating function, different pieces of evolution can be composed together to give well defined quantum unitary evolution with the framework of [37]. Another aspect of the tiling space variable t is that it comes together with its star map t^*, where linear translations on parallel space correspond to oscillations in perpendicular space, which can be seen from Eq. (23) (see also [51]). With the star map, the gauge fixing $t = f(\tau)$ allows for unitary evolution by means of three notions of time – the usual global background time, and the new pair of time parameters, with a clock variable t^*, and a possible global monotonic t parameter, which is the subject of our current research in progress.

To finish we will just touch on the implications for more general dynamics related to the emergence of spacetime structures—essentially, how the underlying tiling spaces and associated partition functions and measures relate to the emergence of inertia and the equivalence principle. Going back to the discussion on emergent gravity and the holographic principle at the beginning of this section, the idea is to understand geodesic motion of particles as a result of an entropic force. Following [1] one introduces a static background with a global timelike Killing vector ξ^a, and considers a generalization of Newton's potential $\varphi = \frac{1}{2}\log(-\xi^a\xi_a)$. Then one can use φ to define a foliation of space, and put general holographic screens at surfaces of constant redshift to consider a force on a particle of mass m close to one screen. The velocity u^a and the acceleration a^b of the particle can be expressed in terms of ξ^a and φ, and in particular the acceleration can be expressed as the gradient $a^b = -\nabla^b\varphi$.

The local temperature T on the screen, using the Davies–Unruh temperature [1], can be defined by

$$T = \frac{\hbar}{2\pi} e^{\varphi} N^b \nabla^b \varphi \tag{32}$$

where N^b is the outward pointing vector normal to the screen and to ξ^b, as the acceleration is perpendicular to the screen. The redshift factor e^{φ} is because the temperature is measured with respect to the reference point at infinity. Leaving the details aside, Eq. (32) brings together thermodynamics on one side (through the temperature) and gravitational force on the other (through the potential), leading to a relativistic analogue of the law of inertia. The right side of Eq. (32) can be interpreted, with the equivalence principle, either in terms of a gravitational field or an accelerated frame of reference, and both views can be seen as emergent phenomena. Our point with this short review of the framework of emergent gravity is to point out the key role of the (somewhat mysterious) correlation between temperature and acceleration (and so gravity), where Eq. (32) is interpreted as telling us the temperature needed to cause a certain acceleration a^b and not the other way around. This picture finds a natural implementation with the short-scale non-ergodic tiling-space-dynamics background. First one considers a transition in tiling space given by Eq. (15) and a probabilistic measure, Eq. (10), from the state sum Eq. (17), for a tiling space of translations of some κ_i vertex type, where the look-savings-ahead algorithm dynamics is such that the ergodic correspondence holds – there is some associated number of clusters dependent on the inflation scale $N(\lambda^n)$, and from Eq. (31) there is a gauge connecting the tiling translation parameter and the relativistic time parameter $t = f(\tau)$. Now consider the same transition, where the savings potential from a look-savings-ahead algorithm leads to a deviation from ergodicity. As the savings potential can give different probability for different paths, it can change t and $N(\lambda^n)$. Specially, we linked $N(\lambda^n)$ with temperature such that the deviation from ergodicity can be connected with a delta in temperature and then, following the entropic gravity approach, with a non-ergodic entropic force. So we have correlated Eq. (32) with a deviation from ergodicity, the quantitative analyses of which we will discuss elsewhere.

5. Conclusions

In this paper we have presented the idea of more general small-scale (time average) probabilistic measures implemented by quasicrystal structures modeled by the model set framework. This procedure is general such that the model set structure can be replaced by other mathematical discrete structures. Our main point on the correspondence given by Eq. (29) is that the small-scale structures must have some imprint on large scale quantum observables to be a meaningful scientific proposal. Our specific construction leads to the possibility of having a specific CPS predicting masses on particle physics, and with a limit on the highest mass that can be measured. This should be well

Preprints (www.preprints.org) | NOT PEER-REVIEWED | Posted: 23 March 2022 doi:10.20944/preprints202111.0359.v2

below the Planck mass, considering the model set structure closer to the Planck scale. This is because in the ergodic correspondence proposed, in the short-distance tiling space side of the correspondence, $I_{\mathcal{T}_\gamma}$ is bounded from above.

In summary, the measure $\mu_{\mathcal{T}^k_\Delta}$ allows one to establish a correspondence between tiling space invariants and intrinsic properties of fundamental physical systems such as the mass discussed above. It can also provide, through the internal tiling space structures, a clock for relational evolution, as well as a delta in temperature for the emergence of inertia and the correspondence principle in the framework of entropic gravity. Gravity as an emergent entropic force, which requires a large number of constituents according to the usual definition of emergence, normally suggests it would be only a classical phenomenon without need for quantization—an aggregate result of microscopic interactions of quantum matter. Here, by contrast, temperature and hence an entropic force can arise for even a single particle with regard to its internal tiling space, making its quantization meaningful. We note that the time average probabilistic measures here considered play a role similar to that of fast variables in [14], or the neural network variables in [52,53]. As future research, model sets may provide one way to reconcile discrete, finite systems with invariance under continuous symmetry groups, addressing the problem "How can discrete, finite systems such as fields on a lattice, display invariance under continuous symmetry groups?" [54]. The novel possibility arises, in terms of spacetime symmetry, by realizing that the discrete and continuous can coexist over LIDS transformations. And in terms of charge gauge symmetry, by generalizing the group G in the CPS $\mathcal{G}$ to more general groups such as the Lie groups necessary for the standard model of particle physics, $SU(3)$, $SU(2)$ and $U(1)$.

As a final note, a non-ergodic substrate for quantum gravity, with an associated non-ergodic causal entropic force, is in line with the ontological hypothesis about the status of reality presented in [43].

Acknowledgments: We thank and acknowledge Dugan Hammock for providing the base code used to test some of the concepts discussed in this paper, such as the CQC model set derived from E_8.

Appendix A. Review of Model Sets

Some properties are representative of model sets $\triangle$, and are necessary to derive the concept of a tiling space. For completeness we review them here, following mainly [15,55].

Appendix A.1. Model Set Properties

Remark A1 (Model set properties)**.** *1. Uniformly discrete: There is a radius $r > 0$ such that each ball of radius r contains at most one point of $\triangle$;*

2. *Relatively dense: There is radius $R > 0$ such that each ball of radius R contains at lest one point of $\triangle$;*
3. *Locally finite: For all compact $\Lambda \subset \mathbb{R}^d$, the intersection $C = \Lambda \cap \triangle$ (called cluster) is a finite or empty set;*
4. *Finite local complexity (FLC): The collection $\left\{(t + \Lambda) \cap \triangle \mid t \in \mathbb{R}^d\right\}$, usually represented by translations $\triangle - \triangle$, contains only finitely many clusters up to translations.*
5. *Uniform distribution: A theorem proved in [15], which says that given some ordering sequence $(x_i)_{i\in\mathbb{N}}$ of the points on $\triangle$, the sequence $(x_i^\star)_{i\in\mathbb{N}}$ is uniformly distributed in K. The star map, $\star$, is given in Eq. (1).*

Point sets with properties 1 and 2 above are called Delone Sets. A characteristic property of a point set in $\mathbb{R}^d$ is the average number of points per unit volume. We are interested in the relative frequency f^r and absolute frequency f^a of sub-sets or clusters of a model set. Due to the uniform distribution property, the relative frequency of a cluster can be computed as a ratio of window volumes

$$f^r_\triangle(C) = \frac{Vol(K_C)}{Vol(K)}, \tag{A1}$$

Preprints (www.preprints.org) | NOT PEER-REVIEWED | Posted: 23 March 2022 doi:10.20944/preprints202111.0359.v2

where K_C is the compact window or coding region of $C \subset \varDelta$, given by $K_C \coloneqq \cap_{x\in C}(K - x^\star)$, and Vol gives the volume of the window. The absolute frequency is given by

$$f^a_\varDelta(C) = dens(\varDelta) f^r_\varDelta(C), \tag{A2}$$

where $dens(\varDelta)$ is the density of the model set, given by

$$dens(\varDelta) = lim_{r\to\infty} \frac{card(\varDelta_r)}{Vol(B_r(0))}, \tag{A3}$$

where for model sets the limit inferior and superior coincide. The open ball of radius r around x is given by $B_r(x)$, and $card$ is the set cardinality.

A hallmark function widely used to characterize a model set is the autocorrelation function

$$\gamma_\varDelta = \sum_{t\in\varDelta-\varDelta} dens(\varDelta) \frac{Vol(K \cap (K - t^\star))}{Vol(K)} \delta_t, \tag{A4}$$

from which the diffraction spectrum can be computed from the Fourier transform

$$\widehat{\gamma_\varDelta} = \sum_{k\in\overline{L}} I(k)\delta_k. \tag{A5}$$

Here $\overline{L} = \pi(\overline{\mathcal{L}})$, with $\overline{\mathcal{L}}$ the dual lattice of $\mathcal{L}$, and the coefficients $I(k) = |A(k)|^2$, which in the case of internal space $\mathbb{R}^d$ is given by

$$A(k) = \frac{dens(\varDelta)}{Vol(K)} \int_K e^{2\pi i(yk^\star)} dy. \tag{A6}$$

In practical application it is useful to use the spherical approximation of the window K, a ball $B_{R_w} = B_{R_w}(0)$ of radius R_w, in spherical coordinates

$$A(k) = \frac{dens(\varDelta)}{Vol(B_{R_w})} \int_{B_{R_w}} e^{2\pi i(yk^\star)} dy = dens(\varDelta) \frac{\Gamma(\frac{d}{2}+1)}{(|k^\star|\pi R_w)^{\frac{d}{2}}} J_{\frac{d}{2}}(2\pi|k^\star|R_w), \tag{A7}$$

where $\varGamma$ is the gamma function, J a Bessel function of the first kind, and the radius of the approximating spherical window is given by

$$R_w = \left(\frac{vol(K)}{\pi^{\frac{d}{2}}} \Gamma(\frac{d}{2}+1)\right)^{\frac{1}{d}}. \tag{A8}$$

Appendix A.2. Model Set Patterns and Tilings

A pattern $\mathcal{T}$ in $\mathbb{R}^d$ ($\mathcal{T} \sqsubset \mathbb{R}^d$) is a non-empty set of non-empty subsets of $\mathbb{R}^d$. The elements of $\mathcal{T}$ are the fragments of the pattern $\mathcal{T}$. For example, a locally finite point set such as $\varDelta$ is naturally turned into a pattern as $\mathcal{T} = \mathcal{T}_\varDelta = \{\{x\} \mid x \in \varDelta\}$.

A tiling in $\mathbb{R}^d$ is another example of a pattern with $\mathcal{T} = \{T_i \mid i \in I\} \sqsubset \mathbb{R}^d$, where I is a countable index set, and such that the fragments T_i of $\mathcal{T}$ are non-empty closed sets in $\mathbb{R}^d$ subject to the conditions

Remark A2 (Tiling conditions)**.** *1.* $\cup_{i\in I} T_i = \mathbb{R}^d$,
2. $int(T_i) \cap int(T_j) = \emptyset$ *for all* $i \neq j$ *and*
3. T_i *being compact and equal to the closure of its interior* $T_i = \overline{int(T_i)}$.

If we release condition 1 above we have a non-space filling tiling as another example of a pattern. The T_i are called regular tiles of the tiling and their equivalence class up to congruence are called prototiles. Recall the locally finite property of point sets from Remark A1. This extends naturally to the pattern $\mathcal{T}$, as does the definition of a cluster $C = \varLambda \sqcap \mathcal{T}$ of $\mathcal{T}$.

Preprints (www.preprints.org) | NOT PEER-REVIEWED | Posted: 23 March 2022 doi:10.20944/preprints202111.0359.v2

Two locally finite patterns $\mathcal{T}$ and $\mathcal{T}'$ are locally indistinguishable (LI), $\mathcal{T} \overset{LI}{\sim} \mathcal{T}'$, when any cluster of $\mathcal{T}$ occurs also in $\mathcal{T}'$ and vice versa. This means that there are translations $t, t' \in \mathbb{R}^d$ such that $\mathcal{T} \sqcap \Lambda = (-t' + \mathcal{T}') \sqcap \Lambda$ and $\mathcal{T}' \sqcap \Lambda = (-t + \mathcal{T}) \sqcap \Lambda$. The translation of a tiling is understood as $t + \mathcal{T} = \{t + T_i \mid i \in I\}$. Locally indistinguishability is an equivalence on the class of patterns, written as $LI(\mathcal{T})$.

A $\mathbb{Z}$-module for a given Λ and $\mathcal{T}$, $Z_\Lambda(\mathcal{T})$, for some $x \in \mathbb{R}^d$, is defined as

$$Z_\Lambda(\mathcal{T}) =< t \mid \mathcal{T} \sqcap (x + \Lambda) = (-t + \mathcal{T}) \sqcap (x + \Lambda) >_{\mathbb{Z}}, \tag{A9}$$

which is the $\mathbb{Z}$-module generated by all translations between occurrences of some Λ-cluster in $\mathcal{T}$. When $\Lambda \subset \Lambda'$, one has $Z_{\Lambda'}(\mathcal{T}) \subset Z_\Lambda(\mathcal{T})$ and $Z_{\Lambda \cup \Lambda'}(\mathcal{T}) = Z_\Lambda(\mathcal{T}) \cap Z_{\Lambda'}(\mathcal{T})$. The limit translation module (LTM) $Z(\mathcal{T})$ is then defined as the inductive limit of the $Z_\Lambda(\mathcal{T})$ over all $\Lambda \subset \mathbb{R}^d$, ordered according to inclusion. The $Z(\mathcal{T})$ is an invariant of $LI(\mathcal{T})$.

A pattern $\mathcal{T}' \sqsubset \mathbb{R}^d$ is locally derivable (LD) from a pattern $\mathcal{T}$, $\mathcal{T} \overset{LD}{\sim} \mathcal{T}'$, when a compact neighborhood $\Lambda \subset \mathbb{R}^d$ of 0 exists such that whenever $(-x + \mathcal{T}) \sqcap \Lambda = (-y + \mathcal{T}) \sqcap \Lambda$ holds for $x, y \in \mathbb{R}^d$, one also has $(-x + \mathcal{T}') \sqcap \{0\} = (-y + \mathcal{T}') \sqcap \{0\}$. This extends to LI classes of patterns. A class $LI(\mathcal{T}')$is called LD from $LI(\mathcal{T})$, $LI(\mathcal{T}) \overset{LD}{\sim} LI(\mathcal{T}')$, when patterns $\mathcal{T}_1 \in LI(\mathcal{T})$ and $\mathcal{T}'_1 \in LI(\mathcal{T}')$ exists such that $\mathcal{T}_1 \overset{LD}{\sim} \mathcal{T}'_1$. This also applies to the point set itself: two model sets obtained from the same CPS, but with different windows K_1 and K_2, satisfy $\triangle(K_1) \overset{LD}{\sim} \triangle(K_2)$ if and only if K_2 can be expressed as a finite union of sets each of which is a finite intersection of translates of K_1, with translations from $L^\star$.

Two patterns $\mathcal{T}_1$ and $\mathcal{T}_2$ (similarly for two LI classes) are called mutually locally derivable (MLD) from each other when $\mathcal{T}_1 \overset{LD}{\sim} \mathcal{T}_2$ and $\mathcal{T}_2 \overset{LD}{\sim} \mathcal{T}_1$. MLD is an equivalence relation on patterns (or LI classes), $\mathcal{T}_1 \overset{MLD}{\sim} \mathcal{T}_2$. It is straightforward to show that with $\mathcal{T} \overset{LD}{\sim} \mathcal{T}'$ one has $Z(\mathcal{T}) \subset Z(\mathcal{T}')$ and with $\mathcal{T} \overset{MLD}{\sim} \mathcal{T}'$ one has $Z(\mathcal{T}) = Z(\mathcal{T}')$. Then the LTM $Z(\mathcal{T})$ of $\mathcal{T}$ is an invariant of the entire MLD class of $LI(\mathcal{T})$.

A pattern $\mathcal{T}$ is translationally repetitive when, for every compact Λ there is a compact $\Lambda' \subset \mathbb{R}^d$ such that for every $x, y \in \mathbb{R}^d$, the relation $\mathcal{T} \sqcap (x + \Lambda) = (-t + \mathcal{T}) \sqcap (y + \Lambda)$ holds for some $t \in \Lambda'$. The set Λ' quantifies the local search space to locate arbitrary Λ-clusters of $\mathcal{T}$. For $\mathcal{T} \overset{LD}{\sim} \mathcal{T}'$, if $\mathcal{T}$ is repetitive, then so is $\mathcal{T}'$.

Finally it is possible to derive a concept of tiling spaces. For simplicity we define the local topology for two FLC sets $\triangle$, $\triangle'$, but it is straightforward to generalise to patterns. So two FLC sets $\triangle$, $\triangle'$ are ε-close when one has $\triangle \cap B_{1/\varepsilon}(0) = (-t + \triangle') \cap B_{1/\varepsilon}(0)$ for some $t \in B_\varepsilon(0)$. The topology is generated by the possible neighborhoods with all $\varepsilon > 0$ sufficiently small. This topology permits the concept of a continuous tiling space $X(\triangle)$ given by $X(\triangle) = \left\{\overline{t + \triangle \mid t \in \mathbb{R}^d}\right\}$, with the closure in the local topology. The discrete tiling space, $X_0(\triangle)$, is given by $X_0(\triangle) = \{\triangle' \in X(\triangle) \mid 0 \in \triangle'\}$.

Appendix A.3. Model Sets Inflation-Deflation Symmetry

To go beyond the "classic" symmetries, one needs an extension of other invariance properties to discrete structures. A discrete structure $\triangle$ is said to have a local inflation-deflation symmetry (LIDS) relative to a linear map L if $\triangle$ and $L(\triangle)$ are MLD, $\triangle \overset{MLD}{\sim} L(\triangle)$. When $L(x) = \lambda_o x$ (or $L(x) = \lambda_o R x$ in general, with R in the orthogonal group, $R \in O(d, \mathbb{R})$), the number λ_o is called the inflation multiplier of the LIDS. A necessary condition for L to define an LIDS is $Z(L(\triangle)) = Z(\triangle)$.

There are different methods to generate LIDS tilings. On concrete method is to consider an inflation rule in one direction, which consists of the homothetic mappings

$$\lambda T_i \mapsto \cup_{j=1}^n T_j + A_{ij} \tag{A10}$$

with finite sets $A_{ij} \subset \mathbb{R}^d$, subject to the mutual disjointness of the interiors of the sets on the right hand side and to the (individual) volume consistence condition $vol(T_i) = \sum_{j=1}^n vol(T_j) card(A_{ij})$, both for each $1 \le i \le n$. In the other direction the inverse map is a consequence of local recognisability [15,56]. For more details on the construction of self-similar aperiodic tilings using inflation/deflation

Preprints (www.preprints.org) | NOT PEER-REVIEWED | Posted: 23 March 2022 doi:10.20944/preprints202111.0359.v2

composition rules see for example [56]. Another method to generate LIDS tilings is by re-scaling the window by an appropriated inflation multiplier as discussed in the main text. Many concrete examples are discussed in [15], see for example [15, Proposition 6.3] for the Penrose–Robinson tiling, [15, Corollary 6.9] for the Danzer's ABCK tiling, [15, Remark 7.7] for the Ammann–Beenker point set and [15, Remark 9.10] for the silver mean chain. Remarkably, if a tiling possesses a LIDS, then the tiling is non-periodic, [15, Theorem 6.3].

Appendix B. 3-Dimensional Compound Quasicrystal from the E_8 Lattice

The *canonical coordinate system* of the E_8-CQC (Compound Quasicrystal) can be given using an *enumeration function*. An enumeration function is an odd and growing function in and on $\mathbb{Z}$

$$f_V : \mathbb{Z} \to \mathbb{Z} | (\forall x \in \mathbb{Z}, f_V(x) = -f_V(-x)) \text{ and } (\forall x, y \in \mathbb{N}^2, f_V(x+y) \geq f_V(x)), \tag{A11}$$

and the *canonical enumeration function* is

$$f_V(x) = \lfloor x\phi \rceil. \tag{A12}$$

The values taken by the function $f_V(\mathbb{Z})$ are given by the integer sequence A007067 in the on-line encyclopedia of integer sequences (OEIS) [57] and its first 20 values are: {0, 2, 3, 5, 6, 8, 10, 11, 13, 15, 16, 18, 19, 21, 23, 24, 26, 28, 29, 31}. The density of $f_V(\mathbb{Z})$ in $\mathbb{Z}$, or the probability of an integer to be in the image of f, is $\delta(f) = \phi^{-1}$. The interval function, or discrete derivative $df_V(x)$, is the palindrome Fibonacci word encoded with Long=2 and Short=1, given by the integer sequence A006340 in the OEIS [57]

$$df_V(x) = f_V(x+1) - f_V(x) = \lfloor (x+1)\phi \rceil - \lfloor x\phi \rceil. \tag{A13}$$

The *canonical coordinate system* of the E_8-CQC is the image of $\mathbb{Z}^3$ by the canonical enumeration function: $f_V(\mathbb{Z}^3)$. In the following we will need the Elser-Sloane conditions:

1. The *canonical planar elimination function* $h(x, y)$ partially encodes the fact that the E_8-CQC is constructed from specific slices of an Elser-Sloane projection of the E_8 Lattice:

$$h(x, y) = h_{x8}(x, y) \equiv 0 \pmod 4 \quad \text{or} \quad h_{y8}(x, y) \equiv 0 \pmod 4, \tag{A14}$$

where

$$h_{x8}(x, y) = (-x + 2y - 3\lfloor x/\phi \rceil - 3\lfloor y/\phi \rceil) \bmod 8, \tag{A15}$$
$$h_{y8}(x, y) = (-3x - 4y - 3\lfloor x/\phi \rceil + 3\lfloor y/\phi \rceil) \bmod 8. \tag{A16}$$

2. The *canonical volumetric elimination function* $h(x, y, z)$ fully encodes the fact that the E_8-CQC is constructed from specific slices of an Elser-Sloane projection of the E_8 Lattice, including the constraints of the planar elimination function as a subset. (Formally, the planar function is redundant, but the volumetric function is more computationally intensive. On large data sets, therefore, it is more efficient to first apply the planar function, and then apply the volumetric function to those vertices that remain.) The volumetric function is given by

$$h(x, y, z) = \begin{pmatrix} -1 & 2 & 0 & -3 & -3 & 0 \\ -1 & -4 & 2 & 1 & 1 & 2 \\ -3 & -4 & 2 & -3 & 1 & -4 \\ -1 & -4 & -4 & 1 & -1 & -2 \\ -1 & 2 & 2 & -1 & -3 & 2 \\ 1 & 2 & 2 & 3 & -3 & 0 \\ -3 & -4 & 0 & -3 & 3 & 0 \\ -3 & 2 & -4 & -3 & -3 & -2 \end{pmatrix} \begin{pmatrix} x \\ y \\ z \\ \lfloor x/\phi \rceil \\ \lfloor y/\phi \rceil \\ \lfloor z/\phi \rceil \end{pmatrix} \equiv (0 \| 4) \pmod 8, \tag{A17}$$

where $(0\|4)$ means a vector whose components are all 0 or all 4, i.e., the 8 components of the resulting vector are either all congruent to 0 modulo 8, or all congruent to 4 modulo 8. The

Preprints (www.preprints.org) | NOT PEER-REVIEWED | Posted: 23 March 2022 doi:10.20944/preprints202111.0359.v2

matrix given in Eq. (A17) is deduced from the orientation of the six dimensional subspace of E_8 projected by the Elser-Sloane projection to the selected 3-dimensional slice in which the point (x', y', z') lives.

3. The *canonical spherical elimination function* $s(x, y, z)$ encodes the fact that the star map image is restricted to a sphere of radius $\phi - 1$

$$s(x, y, z) = \star(x)^2 + \star(y)^2 \star (w)^2 < r^2. \tag{A18}$$

Finally, the model set coordinates x', y', z' in $\mathbb{D}^3$, and the coordinates x", y", z" in $\mathbb{Z}^3$, here called the *crystal proxy*, are deduced from the set $\{x, y, z\}$ by the following bijections between x, x' and x" (and the same for y and z):

$$x'(x) = 10x - \sqrt{20} \star (x) \tag{A19}$$
$$x(x') = \lfloor x'/10 \rceil \tag{A20}$$
$$x"(x) = 10x - \left\lfloor \sqrt{20} \star (x) \right\rceil \tag{A21}$$
$$x(x") = \lfloor x"/10 \rceil \tag{A22}$$
$$x'(x") = 10\lfloor x"/10 \rceil - \sqrt{20} \star (\lfloor x"/10 \rceil) \tag{A23}$$
$$x"(x') = \lfloor x' \rceil. \tag{A24}$$

From the vertices found in the canonical coordinates Eq. (A12), the E_8-CQC is comprised of those selected by Eqs. (A14,A17,A18).

There are further restrictions of possible interest. As a first step, the E_8-CQC-T is a selection from the E_8-CQC of only those vertices forming regular tetrahedrons in the slice (corresponding to regular tetrahedrons in E_8). One way to implement this is an elimination function, applied on $f_V(\mathbb{Z}^3)$, but it is proved that they don't use the full set $f_V(\mathbb{Z})$, so it is more efficient to compose the enumeration function f_V with a second enumeration function g_T, where the composition gives f_T. At the next step, the E_8-CQC-4G is formed by keeping only the "4-groups", the tetrahedrons which meet as a group of four at one common vertex such that their convex hull is a cuboctahedron. We know that they will correspond to the equator of a 24-cell in the E_8 Lattice. Again, one way to implement this is an elimination function, applied now on $f_T(\mathbb{Z}^3)$, but it is more efficient to compose the enumeration function with a new enumeration function g_{4G}, to give f_{4G}

$$\begin{aligned} g_{4G}(x) = ((x \bmod 3) > 0)\left\lfloor \phi^{(x \bmod 3)-3}(5(\lfloor \phi(\lfloor x/3 \rfloor + 1)\rceil - \lfloor \phi \lfloor x/3 \rfloor \rceil) + 3)\right\rceil \\ +5\lfloor \phi \lfloor x/3 \rfloor \rceil + 3\lfloor x/3 \rfloor, \end{aligned} \tag{A25}$$

$$\begin{aligned} f_{4G}(x) = (f_V \circ g_{4G})(x) = f_V(g_{4G}(x)), \\ f_{4G}(x) = ((x \bmod 3) > 0)\left\lfloor \phi^{(x \bmod 3)-3}(8(\lfloor \phi(\lfloor x/3 \rfloor + 1)\rceil - \lfloor \phi \lfloor x/3 \rfloor \rceil) + 5)\right\rceil \\ +8\lfloor \phi \lfloor x/3 \rfloor \rceil + 5\lfloor x/3 \rfloor. \end{aligned} \tag{A26}$$

Note that if we substitute $5, 3, 5$ for 2 and $3, 2, 3$ for 1 in the word Eq. (A13), we obtain $dg_{4G}(\mathbb{Z})$:

$$dg_{4G}(x) = g_{4G}(x + 1) - g_{4G}(x). \tag{A27}$$

Details on python and Wolfram language implementations will be discussed elsewhere.

References

1. Verlinde, E. On the origin of gravity and the laws of Newton. J. High Energ. Phys. 2011, 29 (2011). https://doi.org/10.1007/JHEP04(2011)029.
2. Dieks, D., van Dongen, J., de Haro, S. Emergence in Holographic Scenarios for Gravity, Stud. Hist. Phil. Sci. B **52**, 203-216 (2015). https://doi.org/10.1016/j.shpsb.2015.07.007.
3. Donà, P., Fanizza, M., Sarno, G., Speziale, S. SU(2) graph invariants, Regge actions and polytopes, Class. Quant. Grav. **35**, no.4, 045011 (2018). https://doi.org/10.1088/1361-6382/aaa53a.
4. Steinhaus, S. Coarse Graining Spin Foam Quantum Gravity—A Review, Front. in Phys. **8**, 295 (2020). https://doi.org/10.3389/fphy.2020.00295.

5. Gozzini, F. A high-performance code for EPRL spin foam amplitudes, Classical and Quantum Gravity, (2021). https://doi.org/10.1088/1361-6382/ac2b0b.
6. Ambjørn, J., Jurkiewicz, J., Loll, R. Causal dynamical triangulations and the quest for quantum gravity. In J. Murugan, A. Weltman, G. Ellis (Eds.), Foundations of Space and Time: Reflections on Quantum Gravity (pp. 321-337). Cambridge: Cambridge University Press. https://doi.org/10.1017/CBO9780511920998.013.
7. Cooperman, J. H., Making the case for causal dynamical triangulations, Found Phys 50, 1739–1755 (2020). https://doi.org/10.1007/s10701-015-9972-8.
8. Bombelli, L., Lee, J., Meyer, D., Sorkin, R. D. Space-time as a causal set. Physical review letters, 59(5):521, (1987). https://doi.org/10.1103/PhysRevLett.59.521.
9. Bolognesi, T. Spacetime computing: towards algorithmic causal sets with special-relativistic properties. In Advances in Unconventional Computing, pages 267-304. Springer, (2017). https://doi.org/10.1007/978-3-319-33924-5_12.
10. Wolfram, S. A class of models with the potential to represent fundamental physics, arXiv:2004.08210 [cs.DM], (2020).
11. Gorard, J. Some Relativistic and Gravitational Properties of the Wolfram Model, arXiv:2004.14810v1 [cs.DM], (2020).
12. Arsiwalla, X. D., Gorard, J. Pregeometric Spaces from Wolfram Model Rewriting Systems as Homotopy Types, arXiv:2111.03460 [math.CT], (2021).
13. Leuenberger, G. Emergence of Minkowski-Spacetime by Simple Deterministic Graph Rewriting, arXiv:2110.03388 [gr-qc], (2021).
14. 't Hooft, G. Fast Vacuum Fluctuations and the Emergence of Quantum Mechanics. Found Phys 51, 63 (2021). https://doi.org/10.1007/s10701-021-00464-7.
15. Baake, M., Grimm, U. Aperiodic Order, Cambridge University Press, (2013).
16. Moody, R. V. Model sets: A Survey, (2000). [arXiv:math/0002020 [math.MG]].
17. Senechal, M. J., *Quasicrystals and Geometry*, Cambridge University Press, (1995).
18. Levine, D., Steinhardt, P. J., Quasicrystals. I. Definition and structure. *Phys Review B*, **1986**, *34*, 596, (1986). https://doi.org/10.1103/PhysRevB.34.596.
19. Takakura, H., Gomez, C., Yamamoto, A. et al. Atomic structure of the binary icosahedral Yb-Cd quasicrystal. Nature Mater 6, 58-63 (2007). https://doi.org/10.1038/nmat1799.
20. Amaral, M. M., Aschheim, R., Bubuianu, L., Irwin, K., Vacaru, S. I, Woolridge, D., Anamorphic Quasiperiodic Universes in Modified and Einstein Gravity with Loop Quantum Gravity Corrections, Class. Quant. Grav. **34**, no.18, 185002 (2017). https://doi.org/10.1088/1361-6382/aa828a.
21. Chen, L., Moody, R. V., Patera, J., Non-crystallographic root systems, In: Quasicrystals and discrete geometry. Fields Inst. Monogr, (10), (1995).
22. Koca, M., Koca, R., Al-Barwani, M., Noncrystallographic Coxeter group H4 in E8, J.Phys.,A34,11201 (2001). https://doi.org/10.1088/0305-4470/34/50/303.
23. Koca, M., Koca, N. O., Koca, R., Quaternionic roots of E8 related Coxeter graphs and quasicrystals, Turk.J.Phys.,22,421 (1998).
24. Amaral, M. M., Aschheim, R., Irwin, K. Quantum gravity at the fifth root of unity, Physics Open, 2022, 100098, ISSN 2666-0326, (2022). https://doi.org/10.1016/j.physo.2021.100098.
25. Castro, C. A Clifford algebra-based grand unification program of gravity and the Standard Model: a review study. Canadian Journal of Physics, 92(12): 1501-1527, (2014). https://doi.org/10.1139/cjp-2013-0686.
26. Chester, D., Rios, M., Marrani, A. Beyond the standard model with six-dimensional spacetime, [arXiv:2002.02391 [physics.gen-ph]].
27. Nayak, C., U. Solid State Physics, University of California, (2000).
28. Gómez-León, A., Platero, G., Floquet-Bloch Theory and Topology in Periodically Driven Lattices. Phys. Rev. Lett. 110, 200403, (2013). https://doi.org/10.1103/PhysRevLett.110.200403.
29. Bellissard, J. Gap labelling theorems for Schrödinger's operators. In: From Number Theory to Physics, pp. 538–630, Les Houches March 89, Springer, J.M. Luck, P. Moussa & M. Waldschmidt Eds., (1992). https://doi.org/10.1007/978-3-662-02838-4_12.
30. Walker, K. A universal state sum, (2021). [arXiv:2104.02101 [math.QA]].
31. Amaral, M.; Fang, F.; Hammock, D.; Irwin, K. Geometric State Sum Models from Quasicrystals. Foundations 2021, 1(2), 155-168, (2021). https://doi.org/10.3390/foundations1020011.
32. Kleinert, H. Path integrals in quantum mechanics, statistics, polymer physics, and financial market. 5th edition, World Scientific, (2009).
33. Kuchař, K. V., Time and interpretations of quantum gravity, In G. Kunstatter, D. E. Vincent, and J. G. Williams, editors, *Proceedings of the 4th Canadian Conference on General Relativity and Relativistic Astrophysics*, Singapore, 1992. World Scientific. (1992). https://doi.org/10.1142/S0218271811019347.
34. Isham, C. J., Canonical Quantum Gravity and the Question of Time, In J. Ehlers and H. Friedrich, editors, *Canonical Gravity: From Classical to Quantum*, pages 150–169. Springer-Verlag, Berlin, Heidelberg, (1994). https://doi.org/10.1007/978-94-011-1980-1_6.
35. Anderson, E., The Problem of Time in Quantum Gravity, In V. R. Frignanni, editor, *Classical and Quantum Gravity: Theory, Analysis and Applications*. Nova, New York, (2012).
36. Bojowald, M., Höhn, P. A., Tsobanjan, A. An effective approach to the problem of time: general features and examples, *Phys. Rev. D* 83, 125023, (2011). https://doi.org/10.1103/PhysRevD.83.125023.
37. Amaral, M. M., Bojowald, M. A path-integral approach to the problem of time, Annals Phys. **388**, 241-266 (2018). [arXiv:1601.07477 [gr-qc]]. https://doi.org/10.1016/j.aop.2017.11.027.

38. Kellendonk, J., Sadun, L., Conjugacies of model sets. Discrete and Continuous Dynamical Systems 37, 3805-3830, (2017). http://dx.doi.org/10.3934/dcds.2017161.
39. Sadun, L., Tilings, tiling spaces and topology, Philosophical Magazine 86, 875-881, (2006). https://doi.org/10.1080/14786430500259742.
40. Irwin, K. Toward the Unification of Physics and Number Theory. *Reports in Advances of Physical Sciences*, *3*, 1950003, (2019). https://doi.org/10.1142/S2424942419500038.
41. Langan, C. M. The Cognitive-Theoretic Model of the Universe: A New Kind of Reality Theory. *Progress in Complexity, Information and Design*, 2002.
42. Irwin, K. The Code-Theoretic Axiom: The Third Ontology. *Reports in Advances of Physical Sciences*, *3*, 1950002, (2019). https://doi.org/10.1142/S2424942419500026.
43. Irwin, K.; Amaral, M.; Chester, D. The Self-Simulation Hypothesis Interpretation of Quantum Mechanics. Entropy 2020, 22, 247. (2020). https://doi.org/10.3390/e22020247.
44. Hammock, D.; Fang, F.; Irwin, K. Quasicrystal Tilings in Three Dimensions and Their Empires. Crystals, **2018**, 8, 370. (2018). https://doi.org/10.3390/cryst8100370.
45. Fang, F., Irwin, K. An Icosahedral Quasicrystal and E8 derived quasicrystals. arXiv:1511.07786v2 [math.MG]. (2016).
46. Elser, V., Sloane, N. J. A. A highly symmetric four-dimensional quasicrystal, J. Phys. A, 20:6161-6168, (1987). https://doi.org/10.1088/0305-4470/20/18/016.
47. Dirac, P., A., M., Generalized Hamiltonian dynamics, Can. J. Math. 2 129-148, (1950). https://doi.org/10.4153/CJM-1950-012-1.
48. Rovelli, C., Why Gauge?, Foundations of Physics, 44, no. 1, 91–104, (2014). https://doi.org/10.1007/s10701-013-9768-7.
49. Amaral, M., M., Some remarks on relational nature of gauge symmetry, (2014). http://philsci-archive.pitt.edu/10995.
50. Tegen, R., Relativistic Harmonic Oscillator Potential for Quarks in the Nucleon, Annals Phys. **197**, 439-455 (1990). https://doi.org/10.1016/0003-4916(90)90218-D.
51. Fang, F.; Clawson, R.; Irwin, K. The Curled Up Dimension in Quasicrystals. Crystals, 11, 1238, (2021). https://doi.org/10.3390/cryst11101238.
52. Alexander, S., Cunningham, W. J., Lanier, J., Smolin, L., Stanojevic, S. , Toomey, M. W., Wecker, D. The Autodidactic Universe, (2021). [arXiv:2104.03902 [hep-th]].
53. Vanchurin, V., Towards a theory of quantum gravity from neural networks, (2021). arXiv:2111.00903 [cs.LG].
54. 't Hooft, G. The Black Hole Firewall Transformation and Realism in Quantum Mechanics. Universe. 2021; 7(8):298. arXiv:2106.11152v1 [gr-qc], (2021). https://doi.org/10.3390/universe7080298.
55. Billingsley, P. Probability and measure / Patrick Billingsley Anniversary ed. Wiley series in probability and mathematical statistics. John Wiley & Sons (2012).
56. Solomyak, B. Nonperiodicity implies unique composition for self-similar translationally finite Tilings. Discrete Comput Geom 20, 265–279 (1998). https://doi.org/10.1007/PL00009386.
57. Sloane, N. J. A., Plouffe, S., The Encyclopedia of Integer Sequences, Academic Press, (1995). https://oeis.org/.